HAL

archives-ouvertes.fr

From Excitonic to Photonic Polariton Condensate in a ZnO-Based Microcavity

Feng Li, Laurent Orosz, Olfa Kamoun, Sophie Bouchoule, Christelle Brimont, Pierre Disseix, Thierry Guillet, Xavier Lafosse, Mathieu Leroux, Joël Leymarie, et al.

▶ To cite this version:

HAL Id: hal-00824238

https://hal.archives-ouvertes.fr/hal-00824238

Submitted on 4 Jun 2021

From Excitonic to Photonic Polariton Condensate in a ZnO-Based Microcavity

17 authors, including:

Feng Li
The University of Sheffield
44 PUBLICATIONS   **1,303** CITATIONS

Olfa Kamoun
University of Tunis El Manar
26 PUBLICATIONS   **448** CITATIONS

Christelle Brimont
Université de Montpellier
103 PUBLICATIONS   **1,366** CITATIONS

P. Disseix
Université Clermont Auvergne
83 PUBLICATIONS   **1,327** CITATIONS

Some of the authors of this publication are also working on these related projects:

Project   Gallium Nitride View project

Project   Multifunctional ZnO View project

From Excitonic to Photonic Polariton Condensate in a ZnO-Based Microcavity

Feng Li,[1,2] L. Orosz,[3] O. Kamoun,[4] S. Bouchoule,[5] C. Brimont,[4] P. Disseix,[3] T. Guillet,[4] X. Lafosse,[5] M. Leroux,[1]
J. Leymarie,[3] M. Mexis,[4] M. Mihailovic,[3] G. Patriarche,[5] F. Réveret,[3] D. Solnyshkov,[3] J. Zuniga-Perez,[1] and G. Malpuech[3]

[1]*CRHEA-CNRS, Rue Bernard Gregory, 06560 Valbonne, France*
[2]*Université de Nice Sophia-Antipolis, 06103 Nice, France*
[3]*Institut Pascal, PHOTON-N2, Clermont Université, CNRS and Université Blaise Pascal,*
24 Avenue des Landais, 63177 Aubière cedex, France
[4]*Université de Montpellier 2, CNRS, Laboratoire Charles Coulomb, UMR 5221, 34095 Montpellier, France*
[5]*LPN-CNRS, Route de Nozay, 91460 Marcoussis, France*

We report exciton-polariton condensation in a new family of fully hybrid ZnO-based microcavity demonstrating the best-quality ZnO material available (a bulk substrate), a large quality factor (~ 4000) and large Rabi splittings (~ 240 meV). Condensation is achieved between 4 and 300 K and for excitonic fractions ranging between 17% and 96%, which corresponds to a tuning of the exciton-polariton mass, lifetime, and interaction constant by 1 order of magnitude. We demonstrate mode switching between polariton branches allowing, just by controlling the pumping power, to tune the photonic fraction by a factor of 4.

PACS numbers: 71.36.+c, 03.75.Nt, 78.55.Cr

Cavity exciton-polaritons [1] (polaritons) are the quasiparticles resulting from the strong coupling between photons confined in a microcavity and excitons. Polariton properties have been very extensively studied in the past years, and an impressive set of striking physical phenomena have been demonstrated. One can cite parametric amplification [2] and oscillation [3], bistability [4], and multistability [5,6], Bose-Einstein Condensation in various geometries [7–9], and up to room temperature [10,11], superfluidity [12], topological defect generation, [13–16], Josephson oscillations [17,18], and even magnetricity [19]. These phenomena of very strong fundamental interest can, in principle, serve as a basis for the development of a new generation of optoelectronic devices: polariton lasers [20], polariton switches [21,22], transistors [23] and, ultimately, polariton circuits. Switches and circuits based on polaritons profit from the nonlinearity provided by the exciton-exciton interaction, which is orders of magnitude larger than the one of standard nonlinear crystals. The properties of cavity polaritons are inherited from the properties of their bare constituents, the photon and the exciton, which are two particles very different in nature. Indeed, cavity photons are noninteracting extremely light particles with a lifetime controlled by the quality factor (Q) of the cavity. On the other hand, the exciton mass is 4 orders of magnitude larger than the one of the cavity photon, and they strongly interact with each other. A key principle advantage of cavity polaritons, with respect to their individual constituents, is the possibility to tune their exciton-photon fraction and to completely modify the properties of the polariton single particles as well as of the collective polariton states [24–27]. However, the development of commercial devices exploiting these potentialities requires room

temperature operation, which implies the use of active materials with large exciton binding energy and oscillator strength. This is why attention has turned to wide-band gap inorganic semiconductors, such as GaN and ZnO, and to organic materials [28]. Room temperature polariton lasing, as well as other fundamental effects such as spontaneous symmetry breaking [10] and self-induced Larmor precession [29], was demonstrated in GaN-based microcavities. In ZnO, both exciton oscillator strength and binding energies are much larger than in nitrides [30–32]. As a result, the energy splitting between the polariton eigenmodes can reach 200–300 meV, a record for inorganic structures [33,34]. This feature makes ZnO-based structures an optimum choice for a blue-light- and UV-emitting polariton laser device [35–38]. Another key advantage of such large Rabi splitting values is the possibility to create polariton condensates at positive exciton-photon detuning [37], namely, with a large excitonic nonlinearity fraction, even at room temperature. Following the approach developed in GaN based systems, ZnO-based planar cavities have been fabricated with a bottom epitaxial mirror, an epitaxial ZnO active layer, and a final top dielectric DBR [32,38–40]. Vertical cavity surface emitting lasers [32] and polariton lasers [38,39] were fabricated from such structures, despite a rather low Q (200–600) and strong spatial inhomogeneities. Alternatively, polycrystalline ZnO has been deposited between two dielectric DBRs, thereby sacrificing the crystalline quality of the active material but increasing the cavity Q up to 1000, which has also allowed the observation of polariton lasing up to 250 K [35].

In this Letter we study a new type of microcavity that merges the excellent crystalline properties of bulk ZnO substrates (i.e., defect-free material) with the large Qs of
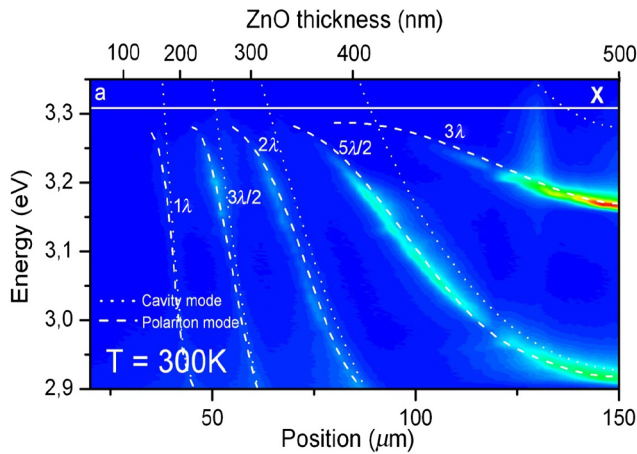
FIG. 1 (color online).   Emission intensity below threshold measured at room temperature along the thickness gradient and showing five LPB when the cavity thickness changes from λ to 3λ. λ is the wavelength corresponding to the excitonic resonance (shown as a solid line). The dashed (dotted) lines show the calculated dispersion of the LPB (bare cavity modes).

enabled by dielectric DBRs (4000 in our sample). As a result, polariton condensates are created in an unprecedented range of parameters: from 4 to 300 K, and for excitonic fractions of the polariton condensate between 17% and 96%. This means that we can create polariton condensates with a broad tuning range of their dispersion and nonlinearities. Furthermore, we demonstrate mode switching allowing, simply by controlling the pumping power, to tune the photonic fraction by a factor 4 (from 7% to 28%).

The studied microcavity is fabricated by etching a ZnO substrate down to a few hundreds of nanometers and by surrounding the remaining ZnO by two HfO_2/SiO_2 distributed Bragg reflectors. This fabrication technique yields a large, quasicontinuous thickness gradient whose value depends on the exact location of the sample, as shown by μPL in Fig. 1. Such a thickness gradient allows for a very large tuning of the energies of the cavity modes and of the

resulting lower polariton branches (LPBs). The curvature of the LPBs as they approach the bare exciton modes evidences clearly the achievement of the strong coupling regime. The fit of these five dispersions, using the transfer-matrix formalism [41], allows us to extract the Rabi splitting, which ranges from 180 to 260 meV (see Supplemental Material [41]), as a function of the active layer thickness. For the following, the exciton-photon detuning as a function of the cavity thickness and the photon-exciton fraction of the polariton modes were estimated within a standard model of coupled oscillators [41].

Polariton condensation is observed in every investigated spot within the microcavity. It is demonstrated by a nonlinear threshold of the μPL emission against pumping. This nonlinear rise of the output intensity, typically of 2 to 4 orders of magnitude, is accompanied by a line sharpening of 1 order of magnitude (down to 0.4 meV) and a moderate blueshift of the LPB energy (typically 1–10 meV, i.e., less than 4% of the actual Rabi splitting). The corresponding data showing condensation at 5, 70, and 300 K, and for various exciton-photon detunings are shown in the Supplemental Material [41]. We do not present here a detailed analysis of the energetic distribution of the emission below threshold (thermalization). We therefore do not claim the achievement of Bose-Einstein Condensation, but the spontaneous formation of a condensate, namely, a macroscopically occupied coherent state. Thanks to the large Rabi splitting value, condensation is observed in a very wide range of parameters between 5 and 300 K, and both for strongly excitonic (96% of exciton fraction) and strongly photonic (83% photon fraction) polaritons. Two representative extreme cases are presented on the same scale in Fig. 2. Below threshold, the excitonlike dispersion is spectrally narrow, being very weakly affected by the photonic inhomogeneous broadening induced by the thickness gradient. On the other hand, the more photoniclike condensate exhibits a large inhomogeneous broadening, with several neighboring modes being visible. The differences are also clear above threshold, with the excitonlike
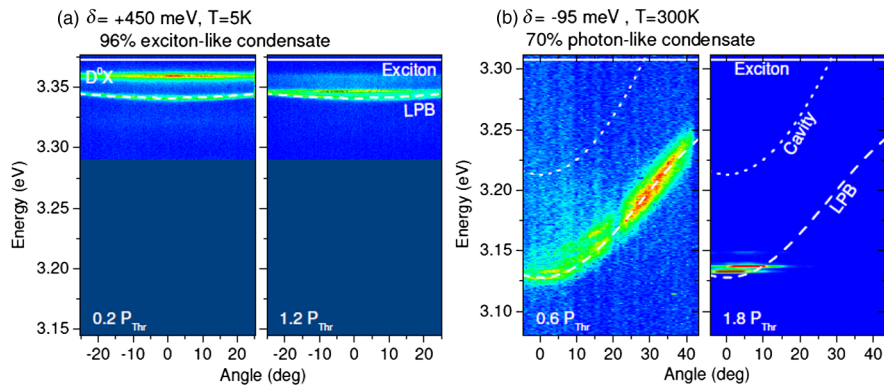

FIG. 2 (color online).   (a) Fourier space images of the emission below (left) and above (right) the condensation threshold for an LPB with a 96% exciton fraction, corresponding to a 2.5λ cavity mode. The data is taken under 130 fs pulsed excitation. Below threshold, the emission consists of the LPB and the nondispersive donor-bound exciton transition (D^0X). (b) Same as (a), but taken under quasicontinuous excitation at 300 K and for a 3λ cavity mode. The photon fraction of the LPB is 70%.

TABLE I.   Range of exciton-photon detunings in which polariton condensation has been achieved and the corresponding extreme exciton-photon fractions.

Temperature (K)	Detuning (meV)	Exciton fraction	Photon fraction
300	+91 to −152	68% to 24%	32% to 76%
250	+118 to −214	72% to 17%	28% to 83%
150	+273 to −132	87% to 26%	13% to 74%
5	+450 to +105	96% to 63%	4% to 37%

condensate appearing well above the LPB dispersion below threshold and being wide in k space due to its interaction with the excitonic reservoir. On the contrary, above threshold the photonic condensate is much less affected by the exciton reservoir, which is localized within the 2 μm pumping laser spot, and, therefore, shows a narrower distribution in k space.

The range of studied exciton-photon detunings where condensation has been achieved, and of corresponding exciton-photon fractions are shown on Table I versus temperature. One can see that properties associated with the exciton fraction (interaction constant) can be tuned by a factor of ~6, whereas properties associated with the photon fraction (mass, lifetime) can be tuned by a factor of ~20. One can therefore create, at will, either strongly interacting condensates with a large lifetime (already more than 10 ps in our structure), or almost interacting-less ones (i.e., more photoniclike states) just by changing the operation temperature (and the detuning).

The dependence of the condensation threshold versus detuning under quasicontinuous excitation and for temperatures ranging from 5 to 300 K is presented in Fig. 3(a). The corresponding theoretical curves, obtained by the numerical solution of semiclassical Boltzmann equations [1,41], are shown in Fig. 3(b). The dependence of the threshold appears quite similar to the one measured in other material systems

[24,25,27]: For a given temperature, the threshold first decreases versus detuning, passes through a minimum and then increases. This optimal detuning is determined by the trade-off between thermodynamics and kinetics. The optimal detuning decreases versus temperature because the kinetics becomes more favorable, contrary to the thermodynamic limit, which degrades. In contrast with the observations in GaN-based cavities [25], and for the same temperature range, the optimal detuning of our ZnO-based structure is positive, as theoretically expected [37]. This behavior is due to the large Rabi splitting value, which induces a very deep energy minimum at the bottom of the LPB while keeping a large density of final states and, therefore, fast relaxation kinetics. Interestingly, the polariton lasing threshold versus detuning at low temperatures shows a double-dip structure [Fig. 3(a), inset]. The existence of a second optimum is induced by efficient polariton scattering directly from the reservoir to the LPB via interaction with an LO phonon, as we recently suggested [39]. At intermediate temperatures (100 K), the two dips merge to form a single minimum, and this is where we obtain the overall lowest pumping threshold. At higher temperature, the optimal detuning value keeps decreasing reaching a value compatible with a relaxation assisted by the emission of 2 LO Phonons. The efficiency of this process allows polariton relaxation towards the LPB despite its large energy offset with respect to the exciton energy. This mechanism, combined with the large density of final states induced by the large Rabi splitting (3 to 5 times larger than in GaN), provides fast scattering rates and is responsible for the low threshold.

A remarkable regime can be achieved in thicker regions of the sample, where several LPBs are present simultaneously. Depending on the above-mentioned trade-off between the thermodynamic (negative detuning) and kinetic (positive detuning) requirements, polaritons "choose" the optimal branch to condense. This is illustrated in Fig. 4(a), where the exciton-photon detuning of
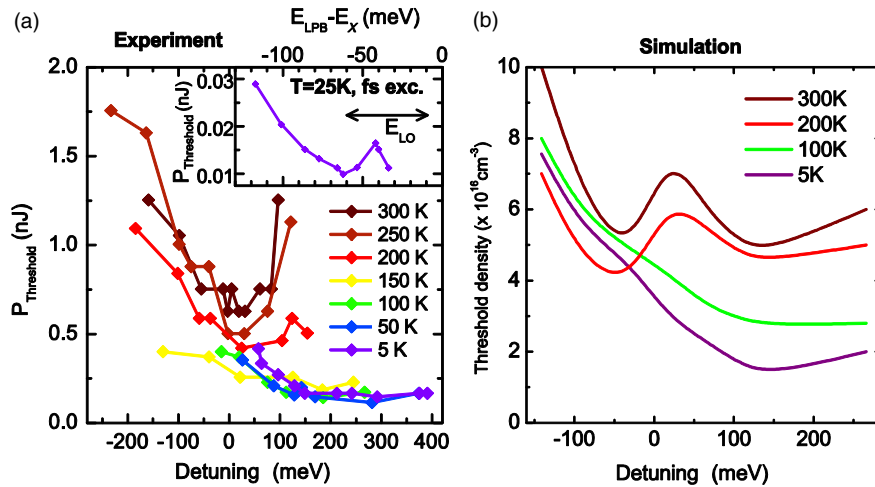

FIG. 3 (color online).   (a) Polariton condensation threshold measured under quasi-continuous excitation, from 5 to 300 K, versus the exciton-photon detuning. The thickness of the cavity is about 2.5λ. Inset: Double dip dependence of the threshold against the offset ($E_{LPB} - E_X$), better revealed by 130 fs pulsed excitation. (b) Polariton condensation threshold density calculated for the same range of parameters as in (a), using the semiclassical Boltzmann equation.

three consecutive LPBs is shown versus the active layer thickness along the gradient. The modes in which polariton condensation takes place are connected with a solid line. While going to less positive detuning [i.e., from left to right in Fig. 4(a)], lasing is continuously observed from the same mode. When the mode becomes too much photoniclike [at a thickness of 913 nm in Fig. 4(a)], the system switches and lasing takes place on the next mode, which is closer to the optimal detuning value and kinetically favored. Furthermore, for a given detuning (comparable to the point at a thickness of 913 nm), the switching can be externally controlled by the pumping, as shown in Figs. 4(b)–4(d). Figure 4(b) (below threshold) shows three polariton modes with very different excitonic contents. Figure 4(c) (at threshold) demonstrates lasing from the intermediate
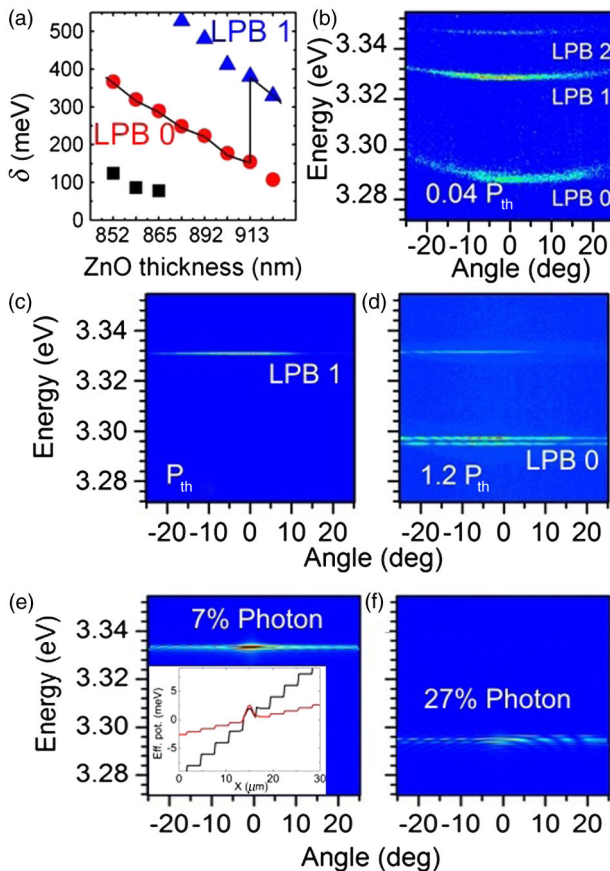

FIG. 4 (color online).   (a) Detuning versus ZnO thickness for three LPB. The solid line binds the modes on which the polariton condensation occurs. The data are taken under 130 fs pulsed excitation at 70 K. (b), (c), (d) Fourier space images illustrating mode switching as a function of pumping intensity (situation similar to point at a thickness of 913 nm in panel (a)). (b) Image below the condensation threshold. (c) Image taken at threshold. Polariton condensation occurs on LPB1 (7% photon). (d) At 1.2 P_{th}, the polariton condensate switches to the mode LPB0 (27% photon). (e), (f) Calculated emission of the polariton condensate created under the 2 μm pumping area and propagating in the potentials shown on the panel (e) (see [41] for details on the simulation). Inset (e) Effective potential seen by the polaritons on LPB1 (red-grey) and LPB0 (black), respectively.

branch LPB1 (7% photon). The relaxation toward this branch is indeed kinetically easier, whereas particles cannot reach the LPB0, which would be more thermodynamically favorable. A further increase of the pumping enhances exciton-exciton scattering processes and the condensate is then able to reach a lower energy state, at the bottom of LPB0, which is 27% photonic [Fig. 4(d)]. This process can be used to realize a tunable laser and is also very promising for room-temperature optical switches as discussed below. Interestingly, the photon fraction of the condensate increases by a factor of 4 by passing from one branch (LPB1) to another (LPB0). This should, in principle, strongly modify the properties of the created condensate and opens a number of possibilities to manipulate them in optical devices.

This modification of properties is clearly visible in our data. The inset of Fig. 4(e) depicts the typical potential seen by the polaritons in both cases. It is composed of a Gaussian potential induced by the excitonic reservoir, which acts on the excitonic part of the polaritons, and a staircase potential induced by the thickness gradient, acting on the photonic part only. The height of a step corresponds to 1 monolayer variation of the cavity thickness. A simulation [41] based on the numerical solution of the modified Gross-Pitaevskii equation [42] using the above-mentioned potential, reproduces very well the observed features [Figs. 4(e) and 4(f)] and gives further insight into the behavior of the condensate in this cavity. The k distribution of the condensate occurring on the LPB1 shows a wide homogeneous peak due to the interaction of the heavy excitonlike polaritons with the localized excitonic reservoir [43]. On the other hand, the more photonic condensate of LPB0 shows a series of discrete well-defined sharp peaks up to large wave vectors values. This is due to the steplike acceleration of the condensed polaritons [44], similar to the one recently evidenced in Ref. [45], where the staircase potential was created by a spatially varying nonresonant pump and was acting on the excitonic part. In the current situation, the condensate propagates along the main thickness gradient, away from the pumping area, and crosses the successive polariton modes associated with the discrete values of the two-dimensional potential. Interestingly, by combining the two types of potentials, acting independently on the photon and on the exciton fractions, one can create a spatial trap for polaritons whose shape would be entirely controlled by the exciton-photon fraction. The condensate could be trapped for a higher exciton fraction and automatically released to a more photonic state when the switching occurs. Then, the released propagating condensate can be used to switch another neighboring condensate. This scheme is very similar to the one recently demonstrated in Ref. [46], but has the advantage of being controlled by a nonresonant optical pump and, ultimately, to be compatible with room temperature operation. Its achievement will however require further investigation on the magnitude of the exciton-exciton interaction in ZnO cavities.

In conclusion, we studied a fully hybrid ZnO cavity combining high material quality and high cavity Q, which allows us to observe polariton condensation from 4 to 300 K and to tune the exciton fraction of the polariton condensate from 17% to 96%. Beyond the technological interest, these new hybrid structures open the very interesting perspective to perform propagation experiments at room temperature and to study the temperature and exciton fraction dependence of the superfluid behavior and topological defects in polariton fluids.

[1] A. Kavokin and G. Malpuech, *Cavity Polaritons*, edited by V. M. Agranovich (Elsevier, North Holland, Amsterdam, 2003).

[2] P. G. Savvidis, J. J. Baumberg, R. M. Stevenson, M. S. Skolnick, D. M. Whittaker, and J. S. Roberts, Phys. Rev. Lett. **84**, 1547 (2000).

[3] R. M. Stevenson, V. N. Astratov, M. S. Skolnick, D. M. Whittaker, M. Emam-Ismail, A. I. Tartakovskii, P. G. Savvidis, J. J. Baumberg, and J. S. Roberts, Phys. Rev. Lett. **85**, 3680 (2000).

[4] A. Baas, J.-Ph. Karr, M. Romanelli, A. Bramati, and E. Giacobino, Phys. Rev. B **70**, 161307 (2004).

[5] T. K. Paraïso, M. Wouters, Y. Léger, F. Morier-Genoud, and B. Deveaud-Plédran, Nat. Mater. **9**, 655 (2010).

[6] D. Sarkar, S. S. Gavrilov, M. Sich, J. H. Quilter, R. A. Bradley, N. A. Gippius, K. Guda, V. D. Kulakovskii, M. S. Skolnick, and D. N. Krizhanovskii, Phys. Rev. Lett. **105**, 216402 (2010).

[7] J. Kazprzak *et al.*, Nature (London) **443**, 409 (2006).

[8] R. Balilli, V. Hartwell, D. Snoke, L. Pfeiffer, and K. West, Science **316**, 1007 (2007).

[9] E. Wertz *et al.*, Nat. Phys. **6**, 860 (2010).

[10] J. J. Baumberg *et al.*, Phys. Rev. Lett. **101**, 136409 (2008).

[11] G. Christmann, R. Butte, E. Feltin, J.-F. Carlin, and N. Grandjean, Appl. Phys. Lett. **93**, 051102 (2008).

[12] A. Amo, J. Lefrère, S. Pigeon, C. Adrados, C. Ciuti, I. Carusotto, R. Houdré, E. Giacobino, and A. Bramati, Nat. Phys. **5**, 805 (2009).

[13] K. G. Lagoudakis, T. Ostatnicky, A. V. Kavokin, Y. G. Rubo, R. Andre, and B. Deveaud-Pledran, Science **326**, 974 (2009).

[14] G. Roumpos, M. D. Fraser, A. Löffler, S. Höfling, A. Forchel, and Y. Yamamoto, Nat. Phys. **7**, 129 (2010).

[15] A. Amo, S. Pigeon, D. Sanvitto, V. G. Sala, R. Hivet, I. Carusotto, F. Pisanello, G. Lemenager, R. Houdre, E. Giacobino, C. Ciuti, and A. Bramati, Science **332**, 1167 (2011).

[16] M. Sich, D. N. Krizhanovskii, M. S. Skolnick, A. V. Gorbach, R. Hartley, D. V. Skryabin, E. A. Cerda-Méndez, K. Biermann, R. Hey, and P. V. Santos, Nat. Photonics **6**, 50 (2011).

[17] K. G. Lagoudakis, B. Pietka, M. Wouters, R. André, and B. Deveaud-Plédran, Phys. Rev. Lett. **105**, 120403 (2010).

[18] M. Galbiati *et al.*, Phys. Rev. Lett. **108**, 126403 (2012).

[19] R. Hivet *et al.*, Nat. Phys. **8**, 724 (2012).

[20] A. Imamoglu and R. J. Ram, Phys. Lett. A **214**, 193 (1996).

[21] A. Amo, T. C. H. Liew, C. Adrados, R. Houdré, E. Giacobino, A. V. Kavokin, and A. Bramati, Nat. Photonics **4**, 361 (2010).

[22] D. Sanvitto *et al.*, Nat. Photonics **5**, 610 (2011).

[23] T. Gao, P. S. Eldridge, T. C. H. Liew, S. I. Tsintzos, G. Stavrinidis, G. Deligeorgis, Z. Hatzopoulos, and P. G. Savvidis, Phys. Rev. B **85**, 235102 (2012).

[24] J. Kazprzak, D. D. Solnyshkov, R. André, L. S. Dang, and G. Malpuech, Phys. Rev. Lett. **101**, 146404 (2008).

[25] J. Levrat, R. Butte, E. Feltin, J. F. Carlin, N. Grandjean, D. Solnyshkov, and G. Malpuech, Phys. Rev. B **81**, 125305 (2010).

[26] M. Aßmann, J.-S. Tempel, F. Veit, M. Bayer, A. Rahimi-Iman, A. Loffler, S. Hofling, S. Reitzenstein, L. Worschech, and A. Forchel, Proc. Natl. Acad. Sci. U.S.A. **108**, 1804 (2011).

[27] E. Wertz, L. Ferrier, D. D. Solnyshkov, P. Senellart, D. Bajoni, A. Miard, A. Lemaıtre, G. Malpuech, and J. Bloch, Appl. Phys. Lett. **95**, 051108 (2009).

[28] S. Kéna-Cohen and S. R. Forrest, Nat. Photonics **4**, 371 (2010).

[29] J. Levrat, R. Butté, T. Christian, M. Glauser, E. Feltin, J.-F. Carlin, N. Grandjean, D. Read, A. V. Kavokin, and Y. G. Rubo, Phys. Rev. Lett. **104**, 166402 (2010).

[30] C. Sheng, G. Wang, W. Zhou, Y. Lin, L. Chernyak, J. Zhao, J. Kong, L. Li, J. Ren, and J. Liu, Nat. Nanotechnol. **6**, 506 (2011).

[31] K. H. Liang, S. F. Yu, and H. Y. Yang, Appl. Phys. Lett. **96**, 101116 (2010).

[32] S. Kalusniak, S. Sadofev, S. Halm, and F. Henneberger, Appl. Phys. Lett. **98**, 011101 (2011).

[33] A. Trichet, L. Sun, G. Pavlovic, N. A. Gippius, G. Malpuech, W. Xie, Z. Chen, M. Richard, and L. S. Dang, Phys. Rev. B **83**, 041302(R) (2011).

[34] W. Xie, H. Dong, S. Zhang, L. Sun, W. Zhou, Y. Ling, J. Lu, X. Shen, and Z. Chen, Phys. Rev. Lett. **108**, 166401 (2012).

[35] H. Franke, C. Sturm, R. Schmidt-Grund, G. Wagner, and M. Grundmann, New J. Phys. **14**, 013037 (2012).

[36] M. Zamfirescu, A. Kavokin, B. Gil, G. Malpuech, and M. Kaliteevski, Phys. Rev. B **65**, 161205 (2002).

[37] R. Johne, D. Solnyshkov, and G. Malpuech, Appl. Phys. Lett. **93**, 211105 (2008).

[38] T. Guillet *et al.*, Appl. Phys. Lett. **99**, 161104 (2011).

[39] L. Orosz *et al.*, Phys. Rev. B **85**, 121201 (2012).

[40] L. Tien-Chang, Y.-Y. Lai, Y.-P. Lan, S.-W. Huang, J.-R. Chen, Y.-C. Wu, W.-F. Hsieh, and H. Deng, Opt. Express **20**, 5530 (2012).

[41] See Supplemental Material at http://link.aps.org/supplemental/10.1103/PhysRevLett.110.196406 for experimental evidence of polariton condensation and numerical methods used to draw the Figs. 3(b), 4(e), and 4(f).

[42] E. Wertz *et al.*, Phys. Rev. Lett. **109**, 216404 (2012).

[43] M. Wouters, I. Carusotto, and C. Ciuti, Phys. Rev. B **77**, 115340 (2008).

[44] B. Sermage, G. Malpuech, A. V. Kavokin, and V. T. Mieg, Phys. Rev. B **64**, 081303 (2001).

[45] M. Aßmann, F. Veit, M. Bayer, A. Löffler, S. Höfling, M. Kamp, and A. Forchel, Phys. Rev. B **85**, 155320 (2012).

[46] D. Ballarini *et al.*, arXiv:1201.4071.